Mediterranean Marine Science

Vol 1, No 2 (2000)

Geochemical characteristics of late Quaternary sediments from the southern Aegean Sea (Eastern Mediterranean)

A. SIOULAS, CH. ANAGNOSTOU, A.P. KARAGEORGIS, C.D. GARBE-SCHONBERG

doi: 10.12681/mms.294

Mediterranean Marine Science
Vol. 1/2, 2000, 119-142

Geochemical characteristics of late Quaternary sediments from the Southern Aegean Sea (Eastern Mediterranean)

A. Sioulas[1], Ch. Anagnostou[2], A.P. Karageorgis[2] and C.-D. Garbe-Schonberg[3]

[1] Hydrobiological Station of Rhodes, Ko Str., 85 100 Rhodes, Greece
e-mail: hsr@rhs.rho.forthnet.gr

[2] National Centre for Marine Research, Institute of Oceanography
Aghios Kosmas, Helliniko, 166 04, Athens, Greece

[3] Universitat Kiel, Institut fur Geowissenschaften, Abt. Geologie
Olshausenstrasse 40, D-24118 Kiel, Germany

Manuscript received: 19 July 1999; accepted in revised form: 1 November 2000

Abstract

Ten cores from the southern Aegean Sea have been logged for their lithological composition and seventy-three sub-samples were analysed for the determination of major and trace elements concentrations. Four lithological units were identified, namely, mud, volcanic, turbidite and sapropel. On the basis of the "Z-2" Minoan ash layer radiocarbon age sedimentation rates for the southern Aegean Sea were estimated at 3.26 to 4.15 cm kyr $^{-1}$. Simple correlation analysis revealed three groups of elements associated with: (1) biogenic carbonates; (2) terrigenous alumino-silicates and (3) sapropelic layers. R-mode factor analysis applied on the carbonate-free corrected data-set defined four significant factors: (1) the "detrital alumino-silicate factor" represented by Si, Al, Na, K, Rb, Zr, Pb and inversely related to Ca, Mg, and Sr; (2) a "hydrothermal factor" loaded with Cr, Ni, Co, Cu, Fe; (3) the "volcanic ash factor" with high loadings for Ti, Al, Fe, Na and (4) a "sapropel factor" represented by Ba, Mo, and Zn. High factor scores for the "hydrothermal factor" were observed in sediment samples proximal to Nisyros Isl., suggesting a potential hydrothermal influence. Red-brown oxides and crusts dredged from this area support further this possibility. The use of factor analysis enabled for a better understanding of the chemical elements associations that remained obscured by correlation analysis.

Keywords: Geochemistry, Factor analysis, South Aegean Sea, Volcanic ash, Sapropel, Turbidite.

Introduction

The Mediterranean Sea is a semi-enclosed marginal sea of long and complex geological history; from west to east it is divided into a series of individual basins that provide relatively uninterrupted sedimentary sequences from the Miocene to the Holocene. Major climatic changes, volcanic eruptions, eustatic and tectonic oscillations have been recorded in the sediments and therefore, the eastern Mediterranean received a con-

siderable amount of attention from marine scientists.

Since the early work of BRADLEY (1938), KULLENBERG (1952) and OLAUSSON (1961) many investigations were concentrated into the recovery and study of organic carbon enriched layers (named as sapropels after KIDD *et al.*, 1978) that were further related to abrupt climatic changes in the eastern Mediterranean. Despite the extensive literature, the depositional processes which have resulted in the sapropels formation, remain unresolved. To date, two theories exist over the sapropel formation mechanism: (a) the anoxia due to stagnation, as a mechanism preserving carbon and (b) the enhanced primary production theory that provides increased carbon flux (for reviews, see CITA & GRIGNANI, 1982; VERGNAUD-GRAZZINI, 1985; ROHLING, 1994, CRAMP & O'SULLIVAN, 1999). The sapropel layers have been extensively described and dated, thus establishing an excellent chronology of the late Quaternary sediment sequence. For example, sapropel S_1 which is the most recently deposited and also common sapropel is da-ted between 5.3 and 9.0 kyr B.P. (THOMSON *et al.,* 1999), while the oldest sapropel S_{12} corresponds to 400,000 yr B.P. (MCCOY, 1974).

Volcanic ash layers in Quaternary sediments of the eastern Mediterranean were first discovered by MELLIS (1954) and initiated the use and refinement of tephrachronology. The ash layers are widespread geographically and may act as stratigraphic markers in order to date the sediment sequences (e.g. NINKOVICH & HEEZEN, 1967; MCCOY, 1974; PICHLER & FRIEDRICH, 1976; THUNELL *et al.*, 1979; MCCOY, 1981; VINCI, 1987; KNOX, 1993). During the last 200,000 yr, 20 widespread ash layers have been deposited over the eastern Mediterra-nean deriving from the Hellenic arc and the Calabrian arc volcanic provinces (KELLER *et al.*, 1978; THUNELL *et al.*, 1979). One of the largest known eruptions in post-glacial time is the Santorini eruption ("Z-2" Minoan ash layer, 1500 yr B.P.). The eruption produced at least 28 km^3 of tephra, deposited over eastern Crete as a 5 cm thick layer, often re-covered in deep-sea cores (WATKINS *et al.*, 1978).

Turbidite and slump deposits interbedded with pelagic sediments are often observed in the eastern Mediterranean and may be readily distinguished with the naked eye (HERMAN, 1972)

The present contribution examines the geochemical composition of core sediments from the southern Aegean Sea and focuses on the differentiation of the Upper-Quaternary sedimentary record into discrete lithological facies according to their geochemical signature. The frequency distribution of major and trace elements are evaluated by R-mode factor analysis and inter-element relations are discussed. In addition, the implication of submarine hydrothermal activity is addressed in order to identify recently active regions.

Area under investigation

The part of the Aegean Sea extending between the Hellenic volcanic arc (Milos, Santorini, Nisyros and Kos Islands) and Crete Isl. determines the boundaries of the working area (Fig. 1). The Aegean is situated on a small, rapidly moving (3.5 cm yr^{-1}, southwest direction) microplate (JACKSON, 1994; DRUITT *et al.*, 1999). The Hellenic volcanic arc formation has resulted from the subduction of the African plate under the Aegean microplate, an activity that currently continues.

The bottom morphology (Fig. 1) is characterised by a narrow continental shelf that extends a few kilometres offshore the islands. The central part of the Cretan Sea is generally deeper than 1000 m, while depths more than 2000 m are encountered in two areas of the eastern part, west of Karpathos Isl.

The sedimentological and geochemical characteristics of the late Quaternary sediments have been described in general by

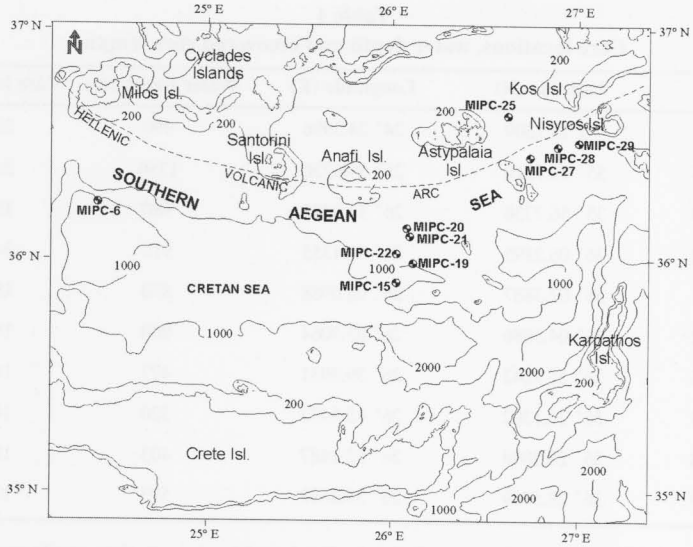

Fig. 1: Working area location, core sampling sites and simplified bathymetry.

Russian scientists who visited the area in the early 60's (for reviews see SHIMKUS, 1981; EMELYANOV & SHIMKUS, 1986). Several "sapropel-like" muds were analysed and their formation was attributed to increased supply of organic detritus to the sea originating in dinoflagellates. Numerous volcanic eruptions mainly of Santorini volcano were identified in a core from the central Cretan Sea, represented by colourless glass (EMELYANOV & SHIMKUS, 1986). Sedimentation rates in the Holocene were estimated at 10-20 cm kyr^{-1} for the central Cretan Sea (SHIMKUS, 1981), reflecting the relatively low sedimentation rates observed over the eastern Mediterranean region.

Materials and methods

Fieldwork was carried out on-board R/V "Aegaeo" during two cruises: (1) from 31/6/1990 to 6/11/1990 and (2) from 7/2/1991 to 2/3/1991. Geophysical data (air-gun profiles and magnetometry) from the area under investigation were used in order to depict areas of interest for core sampling. Selected sites were related to ascending sub-bottom formations accompanied with intense faulting. In this respect a number of thirty-two cores were recovered with a Benthos gravity corer. Core lengths ranged between 0.40 and 4.50 m. All cores were split and logged at the laboratory of the National Centre for Marine Research and ten were selected for further analysis. Selected cores were obtained from three regions: (1) south of Milos Isl.; (2) southeast of Anafi Isl. and (3) the area between the Astypalaia, Kos and Nisyros Isles (for core locations see Fig. 1 and Table 1).

Several smear slides were prepared from each core, approximately in a 10-cm interval, and observed under the polarising microscope in order to obtain a first estimate of the cores' sedimentological characteristics. Core sub-sampling and subsequent geochemical analysis was based upon these observations, across colour changes, and from both sides of lithological boundaries; a number of seventy-two samples were finally selected for bulk geochemistry.

Major elements were determined from 1:5 lithiumborate-mix fused beads by XRF using a PHILIPS PW 1400 spectrometer (C.W. Devey analyst) after pre-ignition of the sample powder at 1000°C. Alpha matrix

Table 1
Core locations, water depth and recovered core length.

Core	Latitude (N)	Longitude (E)	Water Depth (m)	Core length (cm)
MIPC-6	36°15.1309	24° 24.3996	990	235
MIPC-15	35° 51.7210	25° 59.6730	1250	267
MIPC-19	35° 56.7736	26° 13.0495	980	180
MIPC-20	36° 06.2195	26° 08.1355	912	340
MIPC-21	36° 07.3887	26° 08.0988	870	180
MIPC-22	36° 04.3886	26° 03.3064	980	160
MIPC-25	36° 35.9242	26° 39.3931	477	160
MIPC-27	36° 26.1302	26° 45.5473	320	160
MIPC-28	36° 28.2898	26° 52.1487	403	180
MIPC-29	36° 28.5769	26° 59.8693	593	179

factors were used for correcting analytical results.

Trace elements were determined by Inductively-Coupled-Plasma Mass Spectrometry (ICP-MS) using a VG PlasmaQuad 1 instrument after pressurized acid digest. All pressurized acid digestions were performed in SavillexTM 15 ml screw top TeflonTM PFA vials with conventional heating on a hot plate. All acids used were freshly subboiled. HF-$HClO_4$-aqua regia decomposition procedure: 250 mg pulverized and 105°C dried sample were weighed into Teflon vials and moistened with deionized water. Then 4 ml HF and 4 ml freshly prepared aqua regia were added. After ceasing of gas formation vials were closed and taken to 160°C on a hot-plate overnight (>10 hrs). After cooling vials were opened, 1 ml $HClO_4$ added and evaporated at 190°C to incipient dryness. The evaporation step was repeated with addition of 1 ml HNO_3 and a few ml deionized water. Then 1 ml HNO_3 and 5 ml deionized water were added and warmed on a hot plate. This solution was transferred to 50 ml polyethylene sample bottles and made up to 50g total sample weight with deionized water. The resulting digestion solution with 0.5 g l-1 sample concentration (dilution factor = 200) was stored until measurement. Both a blank solution and a sample duplicate were prepared for every batch of ten samples. Carbonate samples were decarbonized by dilute HNO_3 or acetic acid; samples rich in organic carbon were preoxidized by hot concentrated HNO_3 prior to closed vessel digestion. The results presented here were acquired with one single routine-procedure covering the complete element suite. Each sample was acquired in 3 runs and blank-subtracted mean and standard error were calculated. Each calibration was bracketed by a batch of ten samples, comprising: of 1 blank sample, 1 drift control sample (e.g. multielement calibration solution), 1 in-house or international rock standard for accuracy control, 1 duplicate sample which was analysed with a previous sample set and 6 unknown samples. Accuracy, precision and the "real" detection limits for the whole analytical system could be estimated and monitored from the control samples and duplicates. The day-to-day-precision of results estimated from independent duplicate analyses over a long period (2 years) is for most elements better than 2-10%. This is valid for concentrations greater than 10 times the respective detection limit. The instrument was optimised in a first grade to minimize oxide formation. This was achie-

ved by a reduction of nebulizer flow and sample uptake rates and readjustment of the sampling depth (i.e., the distance between sample cone orifice and the load coil). More details of the analytical procedure and instrument set-up as well as results for international standard reference material are given in GARBE-SCHONBERG (1993).

Sediment carbonate content varies considerably (Table 2) and variations in the distribution of other elements are obscured. Therefore chemical elements concentrations have been recalculated on a carbonate-free basis, except for Sr that is primarily associated with carbonates (Table 2). Corre-lation and *R*-mode factor analysis was performed with the statistical package Statigraphics.

Results and Discussion

Lithological units

Late Quaternary sediments of the southern Aegean Sea consist of four major lithological units, namely mud, volcanic, turbidite and sapropel. The lithological units down-core variations are illustrated in Figures 2 to 11, along with the analysed chemical elements vertical distribution.

The *mud unit* is the most common and widespread lithological facies characterised by homogenous thin bedding of yellowish brown to light olive grey silt and clay horizons (muds). The upper part of all cores, except for MIPC-21, consisted of mud. Its thickness varies between 0.1 m (MIPC-27, Fig. 9) and 1.67 m (MIPC-29, Fig. 11); both minimum and maximum thickness of this upper sedimentary unit exists in the same area (Astypalaia, Kos, and Nisyros Isles). The same layer in the core MIPC-28 (Fig. 10), that lies in-between the previous ones, is 0.14 m thick. This irregular sedimentation pattern is related to the bottom morphology, as MIPC-27 and MIPC-28 were recovered from the continental slope and MIPC-29 from a narrow local basin (for water depths see Table 1). The upper mud unit corresponds to the Holocene calcareous marl (ooze) that has been reported over extensive areas of the eastern Mediterra-nean (OLAUSSON, 1961; EMELYANOV & SHIMKUS, 1986; AKSU *et al.,* 1995a; 1995b). The muddy sequence is observed again down-core with similar characteristics and is interrupted by occurrences of the other three lithological units.

The *volcanic unit* is readily recognised as a sandy dark coloured facies. It consists of numerous elongated glass shards and feldspar grains and represents volcanic ash (tephra) horizons deposited during various eruptions of the Hellenic arc volcanoes. The most recent ash layer in the Aegean Sea, 'Z-2' Minoan ash layer (KELLER *et al.,* 1978; WATKINS *et al.*, 1978), has a radiocarbon age of 3370 yr B.P. (PICHLER & FRIEDRICH, 1976). AKSU *et al.* (1995a; 1995b) identified the "Z-2" ash layer in two cores from the eastern Cretan Trough and south of Nisyros Isl., below 7 and 28 cm of Holocene mud, respectively, and estimated the average sedimentation rate at 5.2 cm kyr^{-1}. We identified at least one ash layer in five cores (MIPC-20, MIPC-21, MIPC-27, MIPC-28 and MIPC-29), while two ash layers were identified in cores' MIPC-20 and MIPC-28. On the basis of the cores geographic location, the ash layers down-core depth and the data of AKSU *et al.* (1995a; 1995b), we correlated "Z-2" with the volcanic unit of cores MIPC-27 (at 0.11 m, thickness 10 cm) and MIPC-28 (at 0.14 m, thickness 8 cm). The calculated sediment accumulation rates are 3.26 and 4.15 cm kyr^{-1} and are in close agreement with the values reported by AKSU *et al.* (1995a; 1995b). As the "Z-2" ash layer is always found only a few centimetres under the sea bed (THUNELL *et al.,* 1979; VINCI, 1985; VINCI, 1987) we conclude that ash layers found in cores MIPC-20 (at 1.2 m), MIPC-21 (at 0.98 m) and MIPC-29 (at 1.58 m) are deposits of older eruptions. In respect to the down-core location of these layers we may assume that they correlate to the "Y-2" Cape Riva layer, that

Table 2
Chemical composition (CFB) and summary statistics of southern Aegean Sea lateQuaternary sediments. (continued)

Core	Sampling Depth (cm)	SiO_2 %	TiO_2 %	Al_2O_3 %	Fe_2O_3 %	MgO %	CaO %	Na2O %	K2O %	Cr ppm	Mn ppm	Co ppm	Ni ppm	Cu ppm	Zn ppm	Rb ppm	Sr ppm	Zr ppm	Mo ppm	Ba ppm	Pb ppm
MIPC-6	5-10	38.8	0.80	11.1	5.20	3.98	38.7	1.07	0.46	90	928	19.3	103	53	59	50	831	52	0.9	152	13.9
	45-50	39.7	0.60	11.5	5.66	4.94	33.9	1.40	0.81	109	801	22.2	136	30	66	60	649	58	0.9	155	12.3
	85-90	60.2	0.58	16.7	5.17	9.68	5.7	4.87	2.03	78	1003	14.8	79	21	56	48	779	56	0.8	137	12.0
	103-108	43.7	0.83	12.1	6.58	5.13	27.2	2.26	1.19	134	893	25.0	153	24	68	67	575	66	0.7	197	16.1
	145-150	38.4	0.60	11.1	5.24	5.75	34.5	1.60	0.65	99	810	24.6	136	43	64	52	665	66	0.7	170	12.0
	190-195	39.5	0.59	11.2	5.40	5.51	34.0	1.43	0.61	113	667	22.5	147	36	60	53	664	61	0.8	207	12.5
	205-210	43.5	0.62	12.5	6.16	5.12	27.4	2.26	0.92	110	577	22.2	140	31	72	63	623	80	0.7	298	14.0
	220-225	36.5	0.54	10.5	5.05	4.67	37.7	1.64	0.75	93	776	21.9	117	36	59	49	799	55	1.4	345	11.4
MIPC-15	2-5	28.8	0.45	8.9	4.24	6.10	48.3	0.22	0.28	89	913	16.9	102	34	45	39	796	49	1.2	99	12.6
	10-12	38.3	0.54	11.0	8.76	5.88	34.5	1.32	0.29	113	1897	22.8	114	41	54	47	666	55	2.0	177	11.5
	18-21	35.4	0.53	10.1	4.83	6.34	39.2	1.09	0.69	121	653	19.5	150	29	145	50	638	51	0.6	150	9.3
	39-42	44.5	0.64	11.5	5.45	5.00	27.5	2.58	1.10	98	759	20.0	126	42	62	58	478	104	1.0	200	10.8
	50-55	36.6	0.55	10.9	5.20	5.37	27.9	1.20	0.54	113	1098	20.9	143	30	68	50	636	61	0.7	135	10.0
	85-90	37.5	0.58	11.0	5.64	6.15	35.5	1.21	0.68	133	1338	23.3	168	43	66	53	583	56	0.9	129	10.0
	136-141	ND	ND	ND	ND	ND	ND	ND	ND	90	1210	28.9	124	65	74	47	623	84	0.9	308	11.0
	150-155	28.3	0.48	8.7	4.50	5.92	49.7	0.46	0.32	74	737	13.9	85	24	40	35	756	42	0.6	85	7.9
	167-171	41.8	0.74	13.1	6.88	4.85	28.5	2.36	0.59	102	981	29.9	132	100	68	50	650	75	0.6	292	12.2
	176-180	30.7	0.51	9.3	4.67	5.80	46.1	0.33	0.33	80	655	14.9	91	17	44	39	775	48	0.5	92	9.4
	185-190	ND	ND	ND	ND	ND	ND	ND	ND	65	586	11.4	67	17	43	36	719	45	0.6	85	8.3
	198-203	ND	ND	ND	ND	ND	ND	ND	ND	139	716	24.8	170	139	67	63	529	68	0.6	166	18.4
	208-211	40.2	0.62	11.6	5.64	5.99	31.6	1.82	0.69	118	668	24.3	148	63	63	53	577	66	0.4	174	9.7
	222-225	37.8	0.59	10.8	5.20	6.25	35.3	1.46	0.57	111	831	19.7	137	27	61	50	586	61	0.6	154	9.3
	246-250	46.0	0.61	12.3	6.35	5.61	24.5	2.30	1.04	124	587	24.1	156	35	71	56	525	71	0.6	419	12.0
	265-270	40.2	0.58	10.8	6.56	6.20	32.2	1.60	0.52	115	569	15.3	123	28	53	54	557	58	0.5	164	9.4
MIPC-19	1-5	30.4	0.49	9.3	4.69	6.01	44.8	1.12	0.70	98	920	17.8	114	34	47	41	759	46	1.6	103	3.3
	12-16	31.0	0.47	9.4	4.65	5.91	45.1	0.69	0.32	98	1007	15.5	117	33	46	41	767	45	1.6	107	8.7
	17-19	35.9	0.52	10.6	5.80	5.60	37.1	1.25	0.35	139	4737	26.9	182	42	58	51	790	48	5.2	306	9.9

Table 2
(continued)

Core	Sampling Depth (cm)	SiO_2 %	TiO_2 %	Al_2O_3 %	Fe_2O_3 %	MgO %	CaO %	Na_2O %	K_2O %	Cr ppm	Mn ppm	Co ppm	Ni ppm	Cu ppm	Zn ppm	Rb ppm	Sr ppm	Zr ppm	Mo ppm	Ba ppm	Pb ppm
	19-20	36.8	0.49	9.8	8.58	5.49	33.9	1.64	0.53	136	821	12.8	145	25	62	45	717	44	1.0	290	10.2
	20-23	38.2	0.55	11.3	5.84	5.85	34.9	1.71	0.41	140	338	17.7	177	53	70	37	743	48	3.4	406	10.1
	37-40	37.5	0.56	10.6	5.31	6.45	35.4	1.55	0.99	63	418	9.2	76	13	119	25	285	26	0.3	86	4.9
	160-163	37.7	0.62	11.2	6.13	4.51	34.1	2.56	1.17	49	509	13.2	63	19	30	22	409	31	0.2	303	4.5
	166-170	34.5	0.54	10.3	6.05	5.12	34.7	2.37	1.37	131	611	32.9	191	55	258	48	844	55	19.0	800	10.3
MIPC-20	4-6	42.7	0.59	11.9	5.99	5.98	29.0	2.22	0.74	133	1108	22.1	167	35	60	63	552	75	0.7	195	11.8
	138-140	61.1	0.78	17.2	6.38	2.04	5.0	5.56	2.04	6	5182	17.4	20	14	90	53	206	152	4.2	345	9.5
	199-201	32.5	0.49	9.8	4.96	6.57	43.1	0.75	0.35	113	996	19.0	138	33	48	44	723	52	1.8	113	15.3
	254-256	31.8	0.49	9.6	4.89	6.63	44.0	0.61	0.31	112	994	18.9	140	34	49	42	737	47	1.6	108	14.2
	269-271	60.7	0.48	13.8	4.21	2.15	11.5	4.16	2.77	44	1299	11.1	52	26	59	83	313	212	2.1	358	17.9
	288-290	61.7	0.76	17.5	6.24	2.09	5.6	5.53	1.94	10	4043	15.2	21	15	75	51	213	144	4.2	331	9.1
	318-320	41.8	0.59	11.8	5.88	6.25	29.3	2.11	0.81	138	1063	20.8	177	32	61	58	542	73	0.7	198	11.3
MIPC-21	2-3	31.2	0.46	9.1	4.59	6.53	45.1	0.48	0.30	98	907	16.9	118	30	42	40	742	49	1.4	107	14.2
	17-20	67.2	0.54	15.3	4.18	1.13	3.8	5.26	2.88	10	1151	6.8	8	16	60	84	124	234	2.3	402	14.5
	39-42	39.5	0.57	10.6	5.52	7.03	34.0	1.25	0.67	154	870	21.0	192	27	56	54	595	54	0.5	174	9.9
	47-50	28.9	0.58	10.9	5.96	6.59	33.6	1.72	0.58	113	1070	19.7	148	24	63	45	539	65	0.6	163	9.6
	104-106	44.9	0.49	11.4	5.41	5.08	28.6	2.19	1.11	115	974	18.8	150	23	62	52	565	69	0.7	185	11.1
	109-111	51.0	0.62	13.8	6.05	4.30	18.2	3.08	2.35	104	933	18.9	136	24	77	92	402	165	1.3	211	17.5
	112-114	53.7	0.65	14.7	5.92	3.76	14.6	3.55	2.95	94	931	16.0	119	27	79	114	356	206	1.7	236	20.0
	174-176	43.5	0.80	12.0	6.35	6.88	27.0	1.97	0.85	158	811	26.2	207	41	61	58	500	65	0.6	177	11.6
MIPC-22	5-10	30.8	0.47	9.2	4.68	6.51	45.5	0.27	0.26	98	949	17.5	117	31	45	40	741	44	1.5	105	13.9
	70-75	64.8	0.43	14.0	3.89	1.57	7.3	4.60	3.29	28	627	6.2	31	18	51	85	202	232	1.9	388	16.7
	113-118	67.0	0.42	14.2	3.98	1.25	4.7	5.04	3.43	20	643	5.7	19	20	58	92	146	261	2.1	417	16.9
	124-129	60.2	0.64	16.7	5.17	1.68	5.6	4.87	2.03	6	438	5.1	5	8	33	30	96	85	0.7	174	6.3
	138-142	40.4	0.59	11.5	5.97	7.22	30.9	1.71	0.67	80	500	12.4	103	21	31	29	274	28	0.3	90	5.4
MIPC-25	0-5	32.3	0.44	9.1	4.53	6.58	42.1	1.59	1.02	106	886	17.4	141	26	43	42	756	49	1.2	123	15.2
	23-27	44.6	0.57	12.1	6.39	7.23	25.3	1.88	0.82	207	516	25.6	277	44	68	64	572	62	0.6	294	13.2

Table 2
(continued)

Core	Sampling Depth (cm)	SiO_2 %	TiO_2 %	Al_2O_3 %	Fe_2O_3 %	MgO %	CaO %	Na_2O %	K_2O %	Cr ppm	Mn ppm	Co ppm	Ni ppm	Cu ppm	Zn ppm	Rb ppm	Sr ppm	Zr ppm	Mo ppm	Ba ppm	Pb ppm
	50-55	44.8	0.66	11.8	6.22	5.52	25.7	2.81	1.50	105	893	18.7	144	23	61	47	534	90	0.8	177	10.0
	130-135	34.2	0.43	8.8	4.59	7.23	42.3	0.48	0.42	146	541	18.3	180	20	44	38	751	43	0.5	118	8.6
	155-160	26.3	0.38	7.0	3.94	7.08	50.1	1.08	0.70	102	593	14.2	132	20	123	33	880	38	0.4	80	7.0
MIPC-27	13-16	59.8	0.60	14.3	4.77	2.43	11.1	4.49	2.44	47	894	12.2	98	24	58	68	299	186	1.8	331	19.9
	70-75	25.2	0.30	6.6	3.10	5.29	53.0	1.61	1.26	77	328	9.7	78	14	33	40	1037	70	0.7	74	9.3
	130-135	28.7	0.44	7.6	4.50	5.82	48.7	1.09	0.38	96	356	13.0	96	21	40	22	915	41	0.4	82	6.4
MIPC-28	0-5	31.2	0.44	8.7	4.69	7.58	44.4	0.55	0.38	127	831	18.0	164	26	40	39	753	45	1.3	104	12.6
	15-20	65.5	0.56	14.8	4.30	1.30	4.9	4.99	2.95	19	1066	9.8	21	27	57	81	146	231	2.3	410	17.4
	65-70	43.4	0.44	10.4	4.12	5.41	32.0	1.95	1.32	120	443	16.2	137	21	40	48	684	67	0.8	205	9.5
	120-125	35.8	0.43	9.2	4.89	5.91	40.2	1.13	0.65	102	445	15.3	125	16	41	31	789	53	0.5	219	7.0
	153-157	53.8	0.97	14.9	8.52	4.23	13.3	3.74	1.63	77	931	23.4	94	51	79	47	357	125	2.3	240	9.1
	160-165	ND	ND	ND	ND	ND	ND	ND	ND	86	672	22.1	106	29	60	38	599	98	1.6	265	8.6
	170-175	54.8	1.00	17.0	6.48	3.09	8.0	4.45	1.87	30	850	22.4	35	34	75	41	427	136	1.8	364	9.1
MIPC-29	10-15	41.1	0.54	10.5	6.75	8.01	24.6	2.54	1.45	193	1753	23.5	261	33	56	45	598	58	1.3	127	12.3
	50-55	41.6	0.52	10.6	6.83	8.04	24.4	2.63	1.52	237	596	24.2	336	41	61	54	595	55	6.9	337	9.2
	110-115	43.9	0.56	11.0	6.88	8.09	24.3	2.18	1.32	217	766	23.3	281	26	62	49	549	69	0.7	149	9.5
	140-145	44.9	0.61	11.2	6.90	8.31	24.3	1.91	1.05	237	769	24.6	303	30	70	60	481	60	0.4	156	9.7
	165-170	63.7	0.43	13.6	5.28	2.51	7.8	3.99	3.05	60	561	15.2	69	16	42	86	248	136	2.0	448	15.2
mean		42.3	0.57	11.5	5.52	5.38	29.6	2.20	1.13	103	975	18.5	129	32	63	52	577	81	1.5	218	11.4
median		39.9	0.56	11.1	5.41	5.81	32.1	1.77	0.81	103	826	18.9	132	29	60	49	597	61	0.8	177	10.9
SD		11.1	0.13	2.4	1.10	1.86	13.5	1.44	0.85	49	829	5.8	65	19	30	17	209	55	2.4	125	3.4
min		25.2	0.30	6.6	3.10	1.13	3.8	0.22	0.26	6	328	5.1	5	8	30	22	96	26	0.2	74	4.5
max		67.2	1.00	17.5	8.76	9.68	53.0	5.56	3.43	237	5182	32.9	336	139	258	114	1037	261	19.0	800	20.0

CFB: carbonate free basis; ND: not determined; SD: standard deviation; confidence limits at 95 %

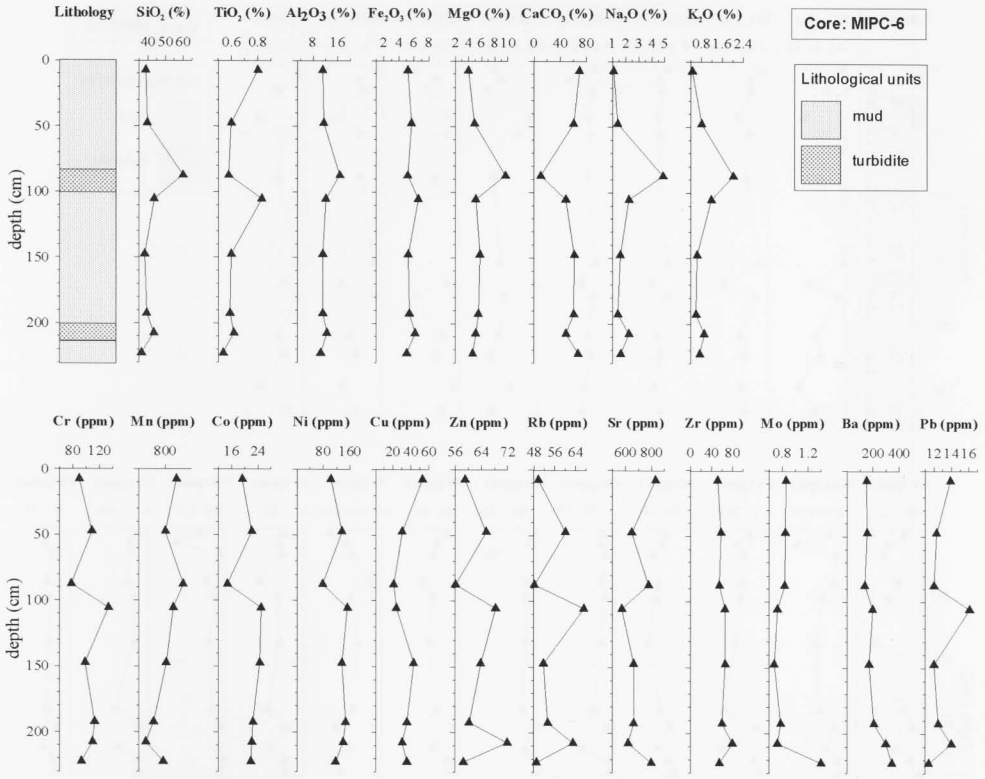

Fig. 2: Lithology and down-core plots of major and trace element concentrations in core MIPC-6. Core location in Fig. 1.

was deposited 18,000 yr B.P. during an eruption of Santorini volcano (VINCI, 1987). The estimated sedimentation rates for this period range from 5.4 to 8.7 cm kyr^{-1}. However, these estimates are lower than the sedimentation rates proposed by EMELYANOV & SHIMKUS (1986) for the Cretan Sea: (1) 10-20 cm kyr^{-1} for the Holocene and (2) 15-20 cm kyr^{-1} for the Upper Wurm (11-30 kyr^{-1}). Finally, the second volcanic ash layer observed at 2.82 m down-core of MIPC-20 may be correlated to the "Y-5" tephra horizon that was deposited approximately 25,000 yr B.P. (THUNELL *et al.*, 1979; VINCI, 1985).

The *turbidite unit* is recognised by bare eye or under the microscope as a mixture of mud with numerous glass shards originating from the volcanic ash layers. Turbidites are found in most of the cores, occasionally more than once, with a thickness varying from a few centimetres to 1.5 m (MIPC-20). Turbidite layers are formed by submarine slides, slumps, debris flows and turbidity currents, mechanisms that carry sediments from the continental slope to the deep ocean-floor. DE LANGE *et al.* (1987) reported the existence of 29 turbidites obtained from two long cores of the Madeira Abyssal Plain (north Atlantic). Based on geochemical characteristics the authors classified the turbidites in: (1) organic-rich; (2) volcanic and (3) calcareous. SACCANI (1986) discriminated the sedimentary sequences of the Cretan Sea in: (1) quartzolithic sand suite derived from the outer arc and (2) lithovolcanic suite derived from the Hellenic volcanic arc. In this respect turbidites of the southern Aegean seem to be related with the second cluster as they were identified by the presence of volcanic ash along the cores.

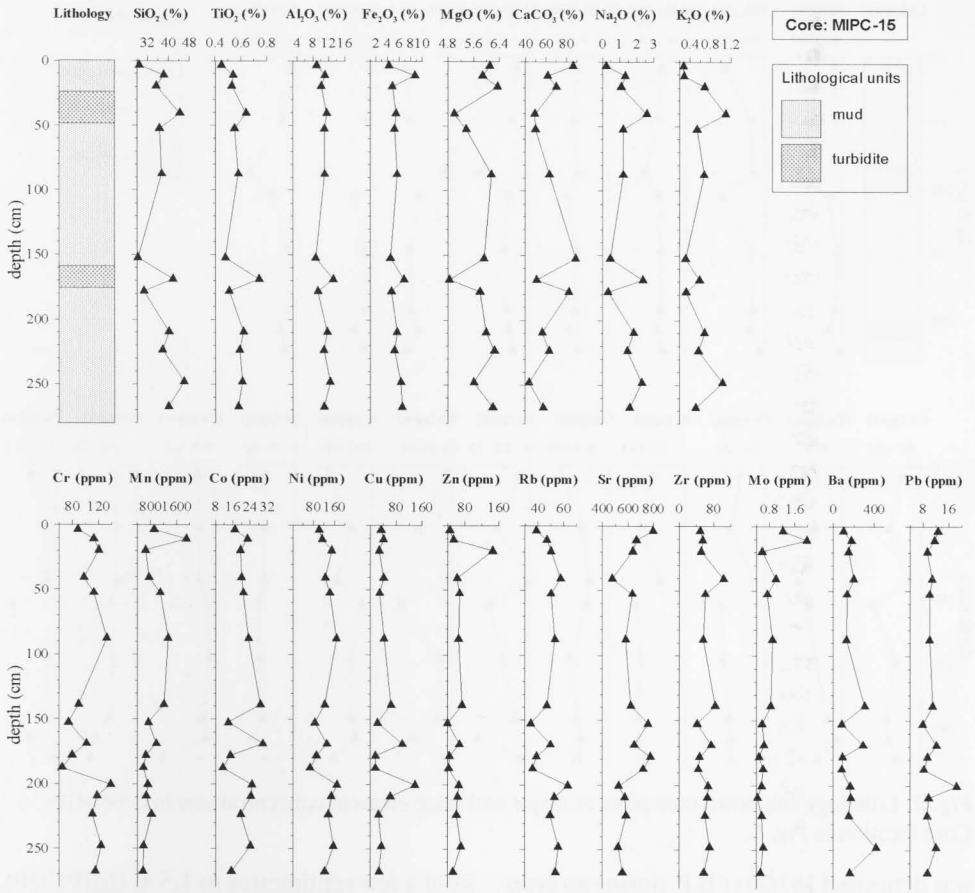

Fig. 3: Lithology and down-core plots of major and trace element concentrations in core MIPC-15. Core location in Fig. 1.

In the central Aegean Sea, LYKOUSIS *et al.* (1995) reported hemipelagic-turbiditic mud sequences in the upper part (0.35-0.45 m) of several cores. Turbidite layers mostly triggered by earthquakes have been identified by X-ray radiography in cores recovered from the deep Ionian Sea (POULOS *et al.*, 1999).

The sapropelic unit is easily recognised due to its characteristic olive black colour, which lies in sharp contrast to the upper and lower sediments. The dark colour results from the elevated organic carbon content that is greater than 2% (e.g. KIDD *et al.*, 1978). Three out of ten cores of the southern Aege-an Sea contained one (MIPC-21, MIPC-27) or more sapropel horizons (three layers in MIPC-19). The sapropel layer thickness in the cores studied varied bet-ween 5 and 12 cm. The upper sapropel unit corresponds to the well-known S_1 sapropel of the eastern Mediterranean (e.g., CRAMP & O'SULLIVAN, 1999; THOMSON *et al.*, 1999) that was deposited between 5.3 and 9.0 kyr B.P. (THOMSON *et al.*, 1999). However, this range may be confined at 7-9 kyr B.P., following the AMS radi-ocarbon dates reported by LYKOUSIS *et al.* (1995) from the central Aegean Sea. It has recently become evident that post-depositional oxidation significantly controls the appearance of S_1 sapropel horizons, removing ap-proximately half or, in some cases, all visual evidence (THOMSON *et al.*, 1995; THOMSON *et al.*, 1999).

Although many cores were recovered from relatively short distances (five cores were col-

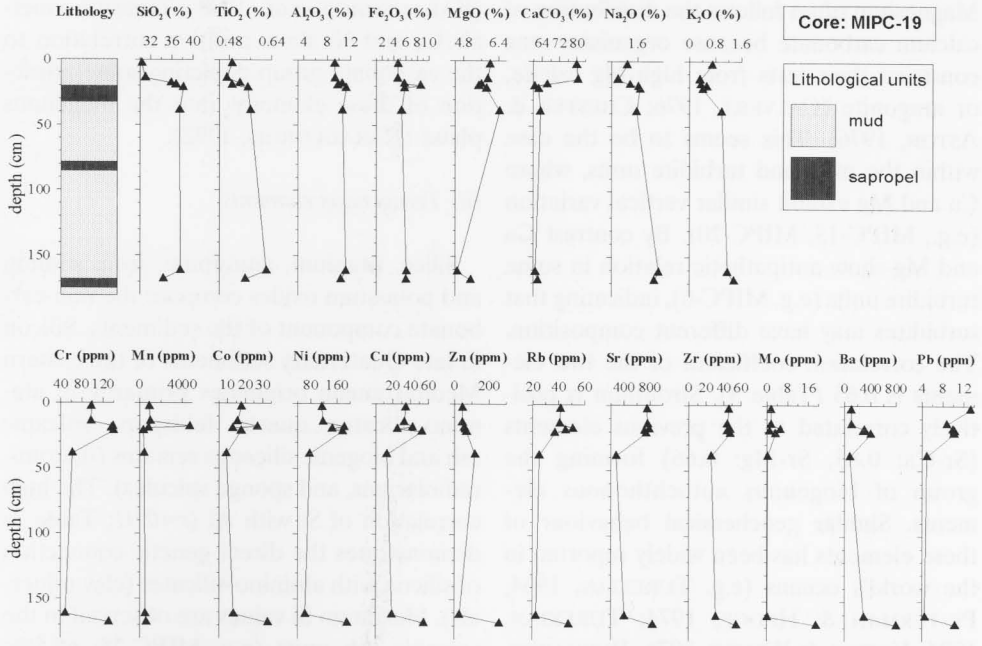

Fig. 4: Lithology and down-core plots of major and trace element concentrations in core MIPC-19. Core location in Fig. 1.

lected southeast of Anafi Isl. and four more southwest of Nisyros Isl., Fig. 1), their lithological structure is highly irregular i.e., in some cases distinct lithological units are completely missing (volcanic ash horizons or sapropels), while others appear in variable thickness (upper mud, tubidites). This pattern is an indication of the high complexity that governed sedimentation processes over the eastern Mediterranean during late Quaternary.

Bulk geochemistry

The southern Aegean Sea sediments show a considerable range of major and trace elements content (Table 2). All measured elements and $CaCO_3$ (calculated from CaO) values down-core distributions are illustrated in Figures 2 to 11.

(i) Carbonates and associated biogenic elements

CaO levels range from 3.8 to 53.0% (Table 2) and the majority of the highest concentrations come from the upper mud unit. Carbonate material originates in the biogenous phase in the form of shell detritus (mostly molluscs and bivalves) or well preserved foraminifera and cocolithofores tests, therefore we may assume that the most of calcium exists in calcium carbonate form. Although carbonate values fluctuate considerably along the cores, a general decrease with depth is observed (e.g. MIPC-15, MIPC-28). Volcanic ash horizons exhibit minimum carbonate content, whilst sapropel horizons show substantial variability; for example, maximum carbonate content appears in the sapropel unit (S_1) of MIPC-27 (Fig. 9), while S_1 in core MIPC-19 contains 66.28, 60.55, and 62.35% CaCO3, respectively (Fig. 4). In general, the late Quaternary sediments analysed are composed of biogenous carbonates in a percentage that exceeds 50% (Table 2).

Magnesium content varies from 1.13 to 8.31% and its distribution is fairly irregular.

Magnesium often follows the distribution of calcium carbonate because organisms may construct their tests from high-Mg calcite, or aragonite (CALVERT, 1976; CHESTER & ASTON, 1976). This seems to be the case within the mud and turbidite units, where Ca and Mg exhibit similar vertical variation (e.g., MIPC-15, MIPC-20). By contrast Ca and Mg show antipathetic relation in some turbidite units (e.g. MIPC-6), indicating that turbidites may have different composition. The correlation coefficient of the two elements is 0.65 (Table 3). Strontium is positively correlated to the previous elements (Sr-Ca: 0.85, Sr-Mg: 0.66) forming the group of biogenous autochthonous elements. Similar geochemical behaviour of these elements has been widely reported in the world's oceans (e.g. TUREKIAN, 1964; PE-TERMAN & HEDGE, 1974; TUREKIAN, 1974; VEIZER & WENDT, 1976, BUCHARDT, 1977; GOREAU, 1977) as well as for central Aegean Sea surface sediments (KARAGEORGIS *et al.,* 1997) and also from Milos Isl. (KARAGEORGIS *et al.,* 1998). Transition metals Cr and Ni show positive correlation to the carbonate group depicting some attraction of these elements into the biogenous phase (KARAGEORGIS, 1992).

(ii) Terrigenous elements

Silica, titanium, aluminum, iron, sodium and potassium oxides compose the non-carbonate component of the sediments. Silicon in late Quaternary sediments of the eastern Mediterranean originates primarily in alumino-silicates, quartz, feldspars, volcanic ash and biogenic siliceous remains (diatoms, radiolarians, and sponge spicules). The high correlation of Si with Al (*r=0.91*; Table 3) demonstrates the direct genetic connection of silicon with alumino-silicates (clay minerals). Maximum Si values are observed in the volcanic ash units (e.g. MIPC-28: 65.5%; MIPC-20: 61.67%; see also Figures 2 to 11 and Table 2) and some turbidites (e.g. MIPC-21: 67.18%), whereas the Al distribu-

Table 3

Correlation coefficients matrix (confidence level at 95%).

	SiO_2	TiO_2	Al_2O_3	Fe_2O_3	MgO	CaO	Na_2O	K_2O	Cr	Mn	Co	Ni	Cu	Zn	Rb	Sr	Zr	Mo	Ba	Pb
SiO_2	1.00																			
TiO_2	0.36	1.00																		
Al_2O_3	0.91	0.62	1.00																	
Fe_2O_3	0.09	0.61	0.28	1.00																
MgO	-0.71	-0.21	-0.62	0.13	1.00															
CaO	-0.98	-0.45	-0.95	-0.22	0.65	1.00														
Na_2O	0.94	0.38	0.90	0.09	-0.72	-0.95	1.00													
K2O	0.89	0.12	0.73	-0.13	-0.73	-0.85	0.89	1.00												
Cr	-0.51	-0.10	-0.50	0.34	0.76	0.45	-0.59	-0.55	1.00											
Mn	0.22	0.25	0.35	0.20	-0.25	-0.25	0.28	0.08	-0.22	1.00										
Co	-0.32	0.40	-0.13	0.52	0.44	0.22	-0.34	-0.45	0.66	0.13	1.00									
Ni	-0.45	-0.06	-0.44	0.33	0.72	0.38	-0.52	-0.48	0.98	-0.18	0.69	1.00								
Cu	-0.19	0.33	-0.05	0.38	0.19	0.15	-0.22	-0.32	0.38	-0.03	0.71	0.40	1.00							
Zn	0.00	0.17	0.07	0.18	-0.01	-0.07	0.10	0.08	0.11	0.06	0.37	0.17	0.24	1.00						
Rb	0.67	0.10	0.51	0.00	-0.50	-0.63	0.54	0.72	-0.11	0.08	-0.05	-0.07	-0.01	0.08	1.00					
Sr	-0.84	-0.37	-0.79	-0.14	0.66	0.85	-0.79	-0.75	0.51	-0.18	0.38	0.44	0.27	0.02	-0.52	1.00				
Zr	0.84	0.14	0.69	-0.15	-0.81	-0.79	0.81	0.90	-0.57	0.17	-0.41	-0.52	-0.20	0.01	0.79	-0.72	1.00			
Mo	0.08	0.02	0.10	0.13	-0.14	-0.12	0.19	0.18	0.04	0.24	0.30	0.12	0.22	0.70	0.08	0.03	0.10	1.00		
Ba	0.54	0.17	0.48	0.20	-0.54	-0.56	0.58	0.55	-0.18	0.15	0.13	-0.10	0.18	0.49	0.43	-0.38	0.51	0.69	1.00	
Pb	0.41	-0.03	0.29	-0.17	-0.37	-0.35	0.29	0.48	-0.12	0.01	-0.04	-0.09	0.08	-0.06	0.78	-0.22	0.61	0.04	0.26	1.00

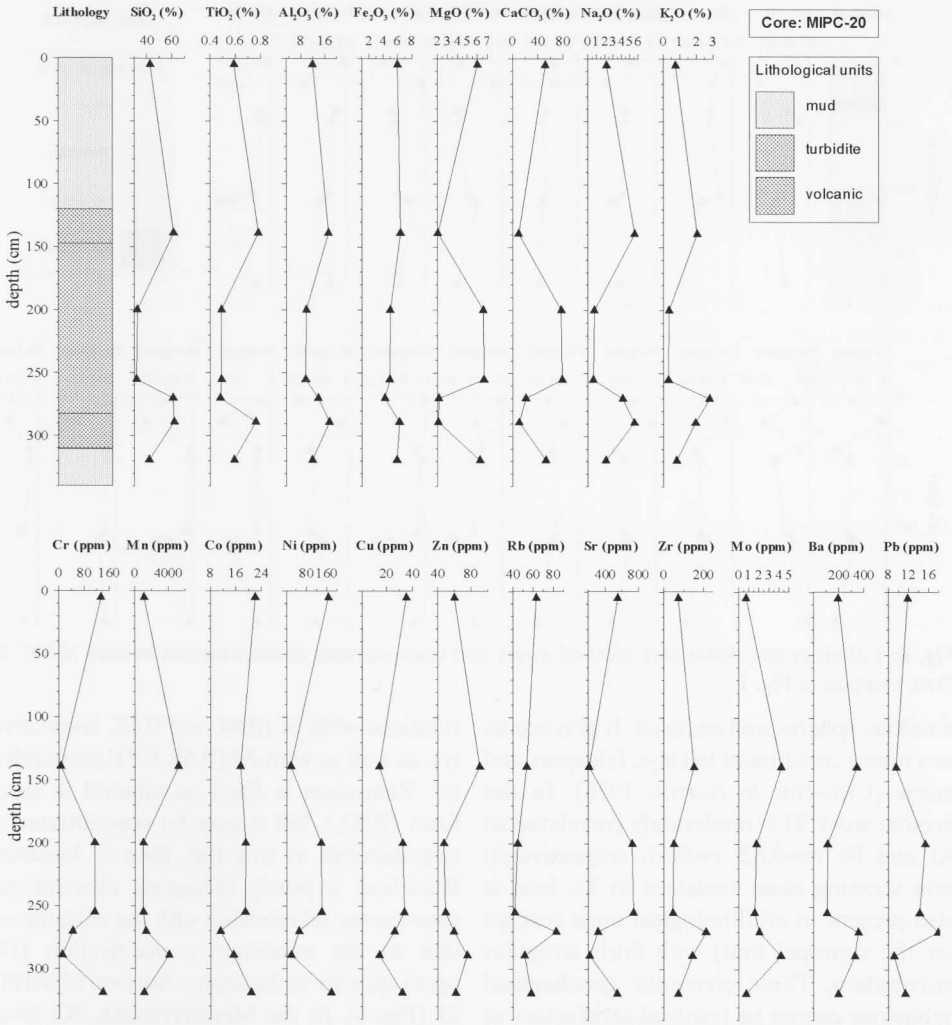

Fig. 5: Lithology and down-core plots of major and trace element concentrations in core MIPC-20. Core location in Fig. 1.

tion shows significant resemblance. In relation to the grain-size, volcanic ash horizons are fairly sandy, meaning that Si and Al are more likely existent in feldspars and volcanic glass/pumice, rather than in fine-grained alumino-silicates.

Titanium as well as aluminum are very immobile in the marine environment, thus may be used for normalisation in order to reduce the variability caused by grain-size or wide range calcium carbonate variations (e.g. HIRST, 1962; KEMP *et al.*, 1974; WINDOM *et al.*, 1989). Due to their conservative behaviour Ti and Al are also indicators of the terrigenous sediment components (e.g. CHESTER *et al.*, 1976; EMELYANOV *et al.*, 1979). Titanium varies from 0.3 to 1% (CFB) and exhibits higher concentrations in the volcanic ash units. Occasionally, turbidite units show high Ti content indicating the presence of Ti in various terrigenous phases. EMELYANOV & SHIMKUS (1986) identified an increasing trend in Ti content from the sand fraction toward the fine silt fraction, Ti being hosted in ilmenite, magnetite and accessory minerals (rutile,

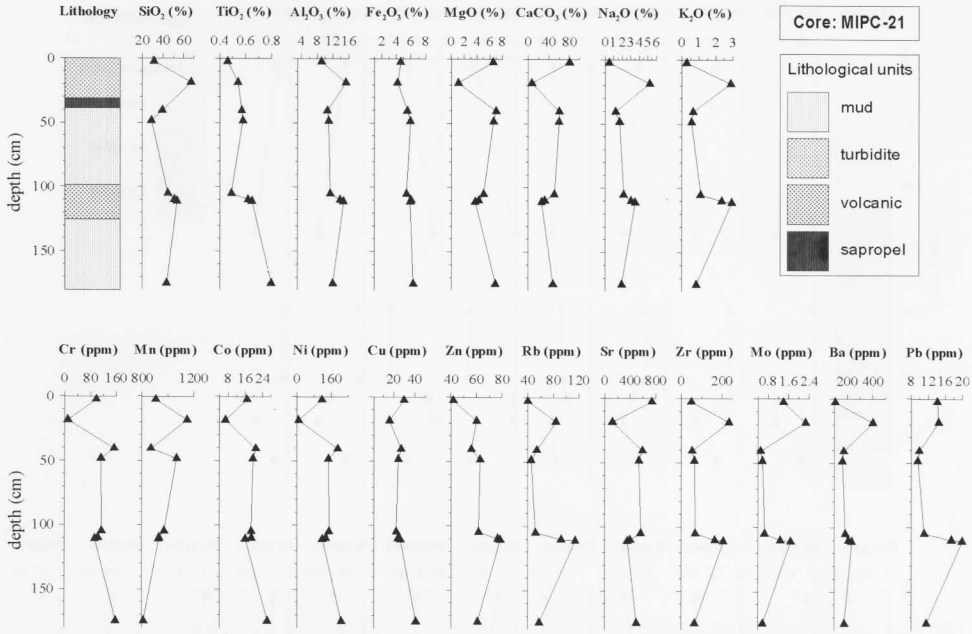

Fig. 6: Lithology and down-core plots of major and trace element concentrations in core MIPC-21. Core location in Fig. 1.

brookite, sphene, and anatase). It also occurs as a minor constituent in clays, feldspars and micas (CHESTER & ASTON, 1976). In the present work Ti is moderately correlated to Al and Fe (*r=0.62; r=0.61*, respectively); iron showing close variation to Ti. Iron is also present in all lithological units (except for the sapropel unit) with fairly irregular distribution. These elements' geochemical behaviour cannot be resolved satisfactory at this point by means of correlation coefficient comparison.

Sodium and potassium are largely associated with the clay minerals in lattice structures and in surface or inter-sheet positions (CHESTER & ASTON, 1976). Amongst the samples analysed, Na and K exhibit very high correlation coefficients with Si and Al (e.g. Na-Si: 0.94; Na-Al: 0.89; K-Si: 0.90, see also Table 3), thus we consider Na and K being incorporated into the alumino-silicates.

A number of trace elements are directly correlated to the terrigenous group, i.e., Zr and Rb. Both elements exhibit positive correlations with Si (0.84 and 0.67, respectively), as well as with Al (0.69, 0.51, respectively). Zirconium is fixed as mineral in oxide form (ZrO_2), but it may be concentrated in clay minerals as smectite, illite or kaolinite. Rubidium is purely lithogenic element and shows some relationship with the volcanic ash unit as the maximum concentration (144 ppm) appears in the tephra horizon of MIPC-21 (Fig. 6). In the Mediterranean, Rb levels are high in the Tyrrhenian Sea, where deposits of the Calabrian volcanic arc are abundant (EMELYANOV & SHIMKUS, 1986). Correlation coefficients of lead with Rb (0.78) and Zr (0.61) indicate that Pb is fixed within the terrigenous phase of the sediments.

(iii) Sapropel associated elements

Molybdenum, barium and zinc form another group of elements exhibiting strong inter-relations, as imposed by their correlation coefficients (e.g. Mo-Zn: 0.70; Ba-Mo: 0.69, Table 3). These elements are associated with the sapropel horizons and display

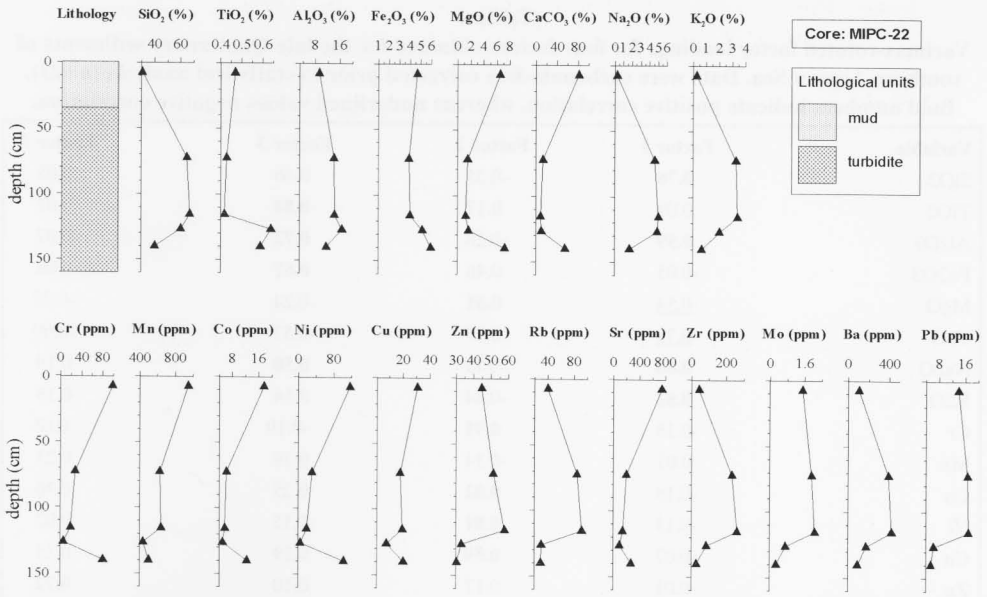

Fig. 7: Lithology and down-core plots of major and trace element concentrations in core MIPC-22. Core location in Fig. 1.

their maxima in the deepest sapropel of MIPC-19 (Mo: 19 ppm; Ba: 800 ppm; Zn: 258 ppm, see also Table 2 and Fig. 4).

Barium concentrations were always found elevated in eastern Mediterranean sapropels (e.g. CALVERT, 1983; SUTHERLAND *et al.*, 1984; THOMSON *et al.*, 1995) and Ba has long been considered as a paleoproductivity proxy (GOLDBERG & *Arrhenius*, 1958; DYMOND *et al.*, 1992; THOMSON *et al.*, 1999; WEHAUSEN & BRUMSACK, 1999). A part of Ba is detrital, while another part is present as discrete barite ($BaSO_4$) crystals <5 microns in size (THOMSON *et al.*, 1995). During the anoxic conditions that prevailed during sapropel formation sulphur was fixed as sulphides and, probably, Mo and Zn precipitate as sulphides (CALVERT, 1983).

Manganese, although not showing any apparent correlation to the sapropel-associated elements Ba, Mo and Zn, has an indirect dependence on them. Mn is reduced to soluble species (Mn^{2+}) when anoxic conditions prevail and therefore, sapropels are formed. In a post-depositional stage, oxygen penetrates the sediment column and remobilises Mn that re-precipitates as oxyhydroxides (Mn^{4+}) in the layers overlying the sapropel. This pattern is illustrated in the elevated Mn concentrations observed over S_1 in cores MIPC-19 and MIPC-21 (Figures 4, and 6, respectively).

(iv) Other trace elements

Trace elements Cr, Co, Ni, and Cu, show relatively high inter-correlation (e.g. Ni-Cr: 0.98; Cu-Co: 0.71; Ni-Co: 0.69), but they don't follow clearly one of the previously defined groups. Therefore, their geochemical behaviour will be assessed with the enhanced statistical procedure of factor analysis.

Factor analysis

Multivariate statistics and in particular factor analysis is a technique that enables grouping of variables (in this case chemical elements) into a number of factors that describe common (geochemical) behaviour. In this way the number of variables under investigation is decreased and interelement

Table 4

Varimax-rotated factor loadings for four factors obtained for the late Quaternary sediments of southern Aegean Sea. Data were carbonate-free corrected prior to statistical analysis (*n=73*). Bold numbers indicate positive correlation, whereas underlined values negative correlation.

Variable	Factor 1	Factor 2	Factor 3	Factor 4
SiO2	**0.78**	-0.35	0.46	0.05
TiO2	0.09	0.17	**0.84**	0.02
Al2O3	**0.59**	-0.28	**0.72**	0.07
Fe2O3	-0.05	0.46	**0.67**	0.08
MgO	-0.54	**0.61**	-0.24	-0.22
CaO	-0.73	0.27	-0.57	-0.09
Na2O	**0.66**	-0.45	**0.50**	0.19
K2O	**0.82**	-0.44	0.14	0.16
Cr	-0.18	**0.91**	-0.19	-0.05
Mn	0.01	-0.14	0.39	0.21
Co	-0.18	**0.82**	0.25	0.30
Ni	-0.13	**0.91**	-0.15	0.02
Cu	-0.07	**0.59**	0.19	0.25
Zn	-0.01	0.17	0.10	**0.72**
Rb	**0.94**	0.09	-0.02	0.05
Sr	-0.60	0.39	-0.49	0.06
Zr	**0.86**	-0.40	0.11	0.11
Mo	0.05	0.08	0.02	**0.90**
Ba	0.48	-0.04	0.20	**0.74**
Pb	**0.75**	0.09	-0.21	0.00
Variance (%)	49.5	19.5	10.2	8.8
Cumulative Variance (%)	49.5	69.0	79.2	88.0

associations may be assessed in greater detail. DAVIS (1986) described effectively the method's principles, whilst numerous investigations be-nefited from its use (SHANKAR *et al.*, 1987; NATH *et al.*, 1989; HODKINSON & CRONAN, 1991; KARAGEORGIS, 1992). R-mode factor analysis with varimax rotation was applied in the carbonate-free sediment concentrations and a four-factor model explaining 88% of the total variance was adopted (Table 4).

Factor 1

Factor 1 accounts for 49.5% of the total data variance (Table 4) and shows a bipolar character. High positive loadings concern Si, Al, Na, K, Rb, Zr, Pb and partly Ba. These elements are incorporated into the terrigenous alumino-silicates and, therefore, this factor can be termed "terrigenous alumino-silicate factor", further corresponding to the "mud lithological unit". The allochthonous detrital phase is opposed to the autochthonous biogenous phase, which is represented by Mg, Ca, and Sr that show negative loadings.

Factor 2

The second factor accounts for 19.5% of the data variance (Table 4) and shows high loadings for a number of metals such as Cr, Co, Ni, Cu and Fe. These elements are associated to hydrothermal processes, thus will be named "hydrothermal factor". Factor scores (Table 5) are higher in the vicinity of Nisyros Isl. (cores MIPC-28, MIPC-29, see

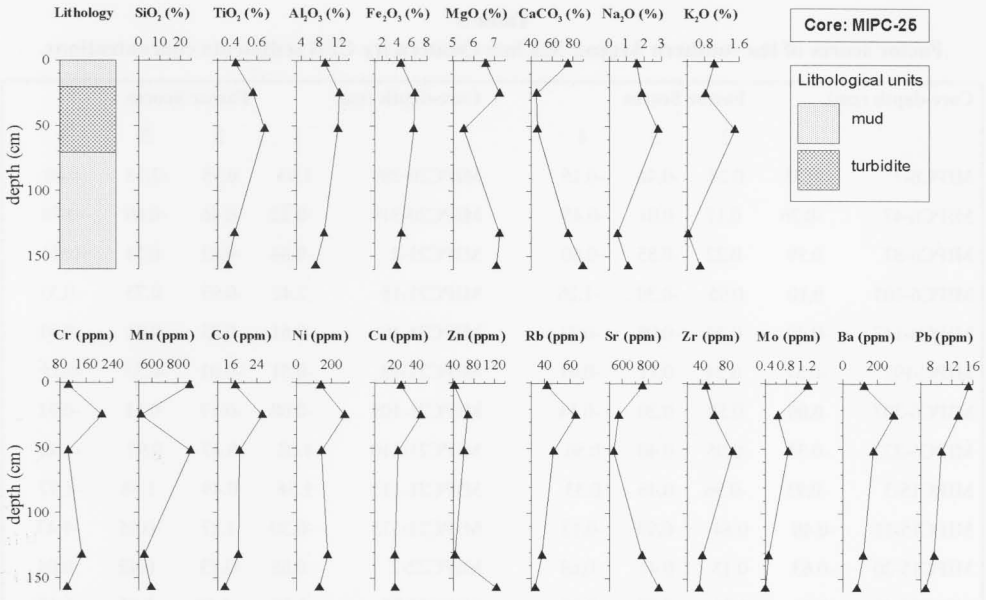

Fig. 8: Lithology and down-core plots of major and trace element concentrations in core MIPC-25. Core location in Fig. 1.

also Fig. 1) where volcanic activity continues until today. Hydrothermal fluids may have been responsible for the accumulation of metal oxides; nevertheless, the absence of Mn participation in this factor is striking. Manganese and iron oxides are important proxies of hydrothermal activity (HODKINSON & CRONAN, 1991; MURPHY *et al.*, 1991). In our four-factor model iron is also represented in factor 3 and manganese distribution is diffused between factors 3 and 4; the latter being controlled primarily by diagenetic re-mobilisation from sapropel layers. Red-brown oxides and crusts that were dredged in Nisyros Isl. area (not ana-lysed in the present study) further support the possibility of modern hydrothermal activity. VARNAVAS' *et al.* (1998) observations are consistent with this opinion, as they reported a submarine hydrothermal system offshore Kos Isl. (see also Fig. 1). Mg and Sr (biogenic elements) show positive loadings with the metals in the "hydrothermal" factor. HODKINSON *et al.* (1994) demonstrated similar relationship from an extensive geochemical study of surface sediments from the Hellenic volcanic arc, but their geochemical association remains unclear.

Factor 3

Factor 3 accounts for 10.2% of the total data variance (Table 4) and shows high loadings for Ti, Al, Fe, Na and also Si and Mn. Factor scores (Table 5) are higher in the samples from volcanic ash horizons, thus can be termed as "volcanic ash factor". It is a second terrigenous factor that shows antipathetic relation to the "biogenic elements" Ca, Mg and Sr, which present negative loadings. Iron and titanium concentrations are often elevated in volcanic sediments (CHESTER & ASTON, 1976; EMELYANOV & SHIMKUS, 1986). DE LANGE *et al* (1987) used Fe and Ti to differentiate turbidites of the Madeira abyssal plain rich in volcanic material that were subsequently named "volcanic turbidites".

Factor 4

The "sapropelic factor" is readily recog-

Table 5

Factor scores of the southern Aegean Sea late Quaternary CFB sediments concentrations.

Core-depth (cm)	Factor Scores				Core-depth (cm)	Factor Scores			
	1	2	3	4		1	2	3	4
MIPC6-7	-0.35	0.24	-0.46	-0.15	MIPC20-289	1.93	0.35	-2.13	1.66
MIPC6-47	-0.26	0.17	0.01	-0.45	MIPC20-319	-0.22	0.46	-0.09	-0.78
MIPC6-87	0.59	-0.22	-0.85	-0.60	MIPC21-2	-0.84	-0.81	0.51	-0.02
MIPC6-105	0.10	0.95	-0.30	-1.26	MIPC21-18	2.42	-0.93	0.75	0.31
MIPC6-147	-0.40	0.30	-0.05	-0.31	MIPC21-40	-0.61	0.25	0.01	-0.81
MIPC-192	-0.37	0.24	0.11	-0.41	MIPC21-48	-0.51	-0.01	-0.53	-0.15
MIPC6-207	0.08	0.58	0.20	-0.54	MIPC21-105	-0.08	-0.17	0.11	-0.31
MIPC6-222	-0.35	0.05	0.40	0.56	MIPC21-110	1.02	0.47	0.97	-1.42
MIPC15-3	-0.93	-0.96	0.46	0.33	MIPC21-113	1.56	0.49	1.56	-1.77
MIPC15-11	-0.48	0.84	-0.99	-0.12	MIPC21-175	-0.30	1.27	-0.65	-1.43
MIPC15-20	-0.63	0.13	0.41	0.65	MIPC22-7	-0.88	-0.73	0.42	0.04
MIPC15-40	0.14	0.26	-0.20	-0.36	MIPC22-73	2.18	-1.18	1.65	-0.12
MIPC15-42	-0.43	-0.04	-0.18	-0.13	MIPC22-115	2.45	-1.11	1.83	-0.09
MIPC15-87	-0.56	0.48	-0.23	-0.47	MIPC22-126	1.53	-1.52	-2.31	0.72
MIPC15-152	-0.93	-1.37	-0.30	0.66	MIPC22-140	-0.34	-0.86	-1.80	-0.09
MIPC15-169	-0.17	1.96	-0.81	-0.45	MIPC25-3	-0.65	-0.75	0.82	-0.22
MIPC15-178	-0.81	-1.24	-0.20	0.39	MIPC25-25	-0.46	1.55	0.69	-1.74
MIPC15-210	-0.40	0.74	-0.38	-0.55	MIPC25-52	0.11	0.15	-0.68	-0.36
MIPC15-223	-0.45	-0.16	-0.33	-0.19	MIPC25-132	-1.09	-0.68	0.33	-0.28
MIPC15-248	0.08	0.94	0.04	-0.35	MIPC25-157	-1.18	-1.08	0.65	1.36
MIPC15-267	-0.34	-0.12	-0.59	-0.46	MIPC27-14	1.66	-0.29	0.93	-0.55
MIPC19-3	-0.74	-0.64	0.39	0.11	MIPC27-72	-0.87	-2.30	1.22	0.88
MIPC19-14	-0.86	-0.81	0.00	0.48	MIPC27-132	-1.11	-1.51	-0.25	0.86
MIPC19-18	-0.57	1.24	-0.09	1.17	MIPC28-3	-1.04	-0.63	0.57	-0.31
MIPC19-19	-0.49	0.25	-0.42	0.00	MIPC28-17	2.30	-0.60	1.01	-0.01
MIPC19-21	-0.55	0.79	0.33	0.66	MIPC28-67	-0.26	-0.78	0.56	-0.12
MIPC19-38	-0.31	-1.04	-1.31	1.29	MIPC28-123	-0.73	-1.02	-0.05	0.56
MIPC19-162	-0.03	-0.86	-1.81	1.03	MIPC28-155	0.84	1.68	-2.31	-0.17
MIPC19-168	-0.20	3.81	3.08	5.73	MIPC28-173	1.34	0.92	-2.29	0.67
MIPC20-5	-0.16	0.55	-0.05	-0.86	MIPC29-12	0.24	1.60	1.26	-0.78
MIPC20-139	2.01	0.63	-2.23	1.93	MIPC29-52	-0.62	2.03	1.09	-0.57
MIPC20-200	-0.76	-0.37	0.56	-0.28	MIPC29-112	0.54	2.18	0.04	-0.92
MIPC20-255	-0.85	-0.40	0.45	-0.16	MIPC29-142	-0.64	1.44	0.04	-2.05
MIPC20-270	1.81	-0.61	1.48	-0.18	MIPC29-168	1.67	-0.34	1.23	-0.38

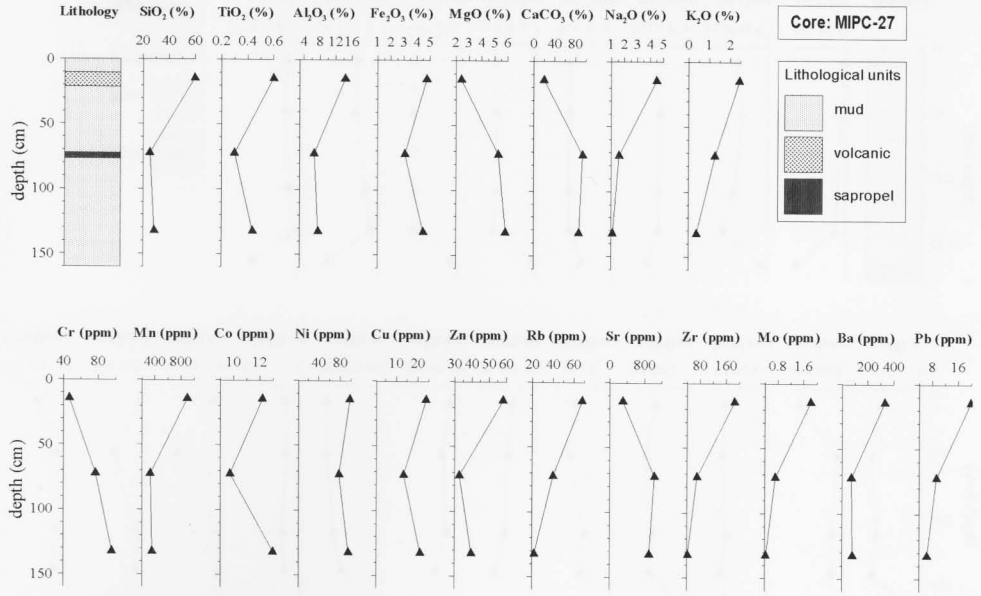

Fig. 9: Lithology and down-core plots of major and trace element concentrations in core MIPC-27. Core location in Fig. 1.

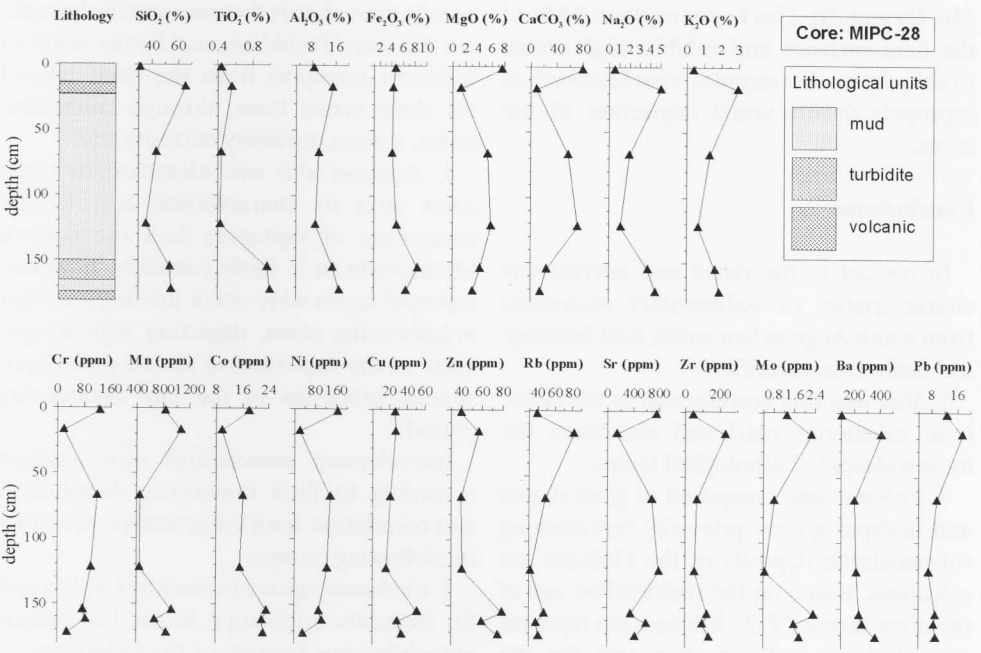

Fig. 10: Lithology and down-core plots of major and trace element concentrations in core MIPC-28. Core location in Fig. 1.

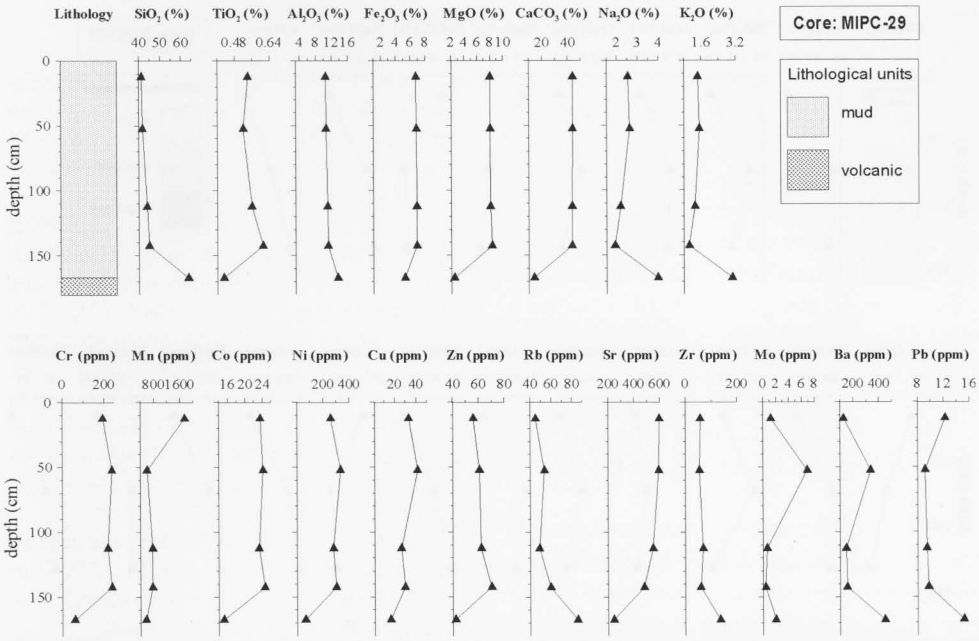

Fig. 11: Lithology and down-core plots of major and trace element concentrations in core MIPC-29. Core location in Fig. 1.

nised from the exclusively high loadings of Mo, Ba and Zn. This factor explains 8.8% of the data variance and exhibits high scores (Table 5) in the samples characterised as sapropels during visual inspection of the cores.

Conclusions

In respect to the visual and microscopic characteristics of sedimentary sequences from south Aegean Sea cores, four lithological units were identified:

1. *Mud unit* that corresponds to the Holocene calcareous marl and comprises the most widespread lithological facies.

2. *Volcanic unit* composed of glass shards and feldspar grains, primarily representing volcanoclastic deposits of the Hellenic arc volcanoes. Based on the radiocarbon age of the most recent "Z-2" Minoan ash layer we estimated the sedimentation rate for the upper Holocene period at 3.26 to 4.15 cm kyr^{-1}.

3. *Turbidite unit* is a melange of silt and clay with components of the volcanic unit, usually glass shards that are spread throughout the core. Turbidites may be the result of sediment transport from the shelf toward the deep ocean floor, through submarine slides, slumps, turbidity currents, etc.

4. *Sapropel unit* was identified in three cores after its characteristic colour. The occurrence of sapropels over the eastern Mediterranean is fairly common; however, sapropel layers were often missing amongst neighbouring cores, depicting high irregularity of the depositional and/or post-depositional processes of the late Quaternary period.

Interelement associations were studied according to their down-core distribution and correlation coefficient matrix, revealing the following groups:

1. *Carbonates group* formed by Ca, Mg and Sr, elements originating in the bio-genous autochthonous fraction of the sediments.

2. *Terrigenous group* composed of Si, Ti, Al, Fe, Na, K, Zr, Rb and Pb, elements originating in the detrital alumino-silicates

(mainly clay minerals) and the volcanoclastic material.

3. *Sapropel group* represented by Mo, Ba and Zn, characteristic elements of the eastern Mediterranean sapropels and, therefore, related to elevated organic carbon content.

Using multivariate statistics (factor analysis) applied in the carbonate-free corrected data set, we defined a four-factor model that explains effectively 88% of the data variance. The use of factor analysis proved to be effective in the identification of element associations that were not resolved by visual-microscopic examination or correlation analysis. The factors defined are the following:

1. The *"detrital alumino-silicates factor"* is the most important factor integrating the elements of the *terrigenous group* as well as a part of Ba. The elements of the *carbonates group* are inversely correlated to the *terrigenous group* elements, due to the antipathetic relationship of the detrital versus biogenous phases.

2. The *"hydrothermal factor"* associates Cr, Co, Ni, Cu and Fe, elements related to potential hydrothermal processes. High factor scores were identified in the Nisyros Isl. cores, indicating a possible hydrothermal influence in this area.

3. The *"volcanic ash factor"* shows high loadings for Ti, Al, Fe, Na, Si and Mn. The elements reflect the composition of volcanic ash horizons rich in glass shards and feldspars originating in the products of the Hellenic arc volcanic eruptions.

4. The *"sapropel factor"* involves Mo, Ba and Zn elements related to the sapropel layers identified in the cores.

Acknowledgements

This research received support from the project MIPAMEHR (Modular Instrument Package and its Application in Mediterranean Hydrothermal Research) funded by the EC under programme MAST-1.

References

AKSU, A.E., YASAR, D., & MUDIE, P.J., 1995a.Paleoclimatic and paleoceanographic conditions leading to development of sapropel layers S1 in the Aegean Sea. *Palaeogeogr. Palaeoclimatol. Palaeoecol.,* 116, 71-101.

AKSU, A.E., YASAR, D., & MUDIE, P.J., 1995b. Origin of glacial - Holocene hemipelagic sediments in the Aegean Sea: clay mineralogy and carbonate cementation. *Mar. Geol.,* 123, 33-59.

BRADLEY, W.H., 1938. Mediterranean sediments and Pleistocene Sea levels. *Science*, 88, 376-379.

BUCHARDT, B., 1977. Oxygen isotope ratios from shell material from the Danish Middle Paleocene (Selandian) deposits and their interpretation as paleotemperature indicators. *Paleogeogr., Paleoclimatol., Paleoecol.*, 22, 200-209.

CALVERT, S.E., 1976. The mineralogy and geochemistry of near-shore sediments. In: J.P.,Riley & R., Chester (Eds), Chemical Oceanography. Academic Press, New York, 187-280.

CALVERT, S.E., 1983. Geochemistry of Pleistocene sapropels and associated sediments from the Eastern Mediterranean. *Oceanol. Acta,* 6, 255-267.

CHESTER, R., & ASTON, S.R., 1976. The geochemistry of deep-sea sediments. In: J.P., Riley & R., Chester (Eds), Chemical Oceanography. Academic Press, New York, 6, 281-390.

CHESTER R., ASTON S.R., & BRUTY D., 1976. The trace element partition geochemistry in an ancient deep-sea sediment core from Bermuda Rise. *Mar. Geol.,* 21, 271-288.

CITA, M.B., & GRIGNANI, D., 1982. Nature and origin of late Neogene Mediterranean sapropels. In: S.O., Schlanger & M.B., Cita (Eds.), Nature and Origin of Cretaceous Carbon-Rich Facies. Academic Press, San Diego, CA, 165-196.

CRAMP, A., & O'SULLIVAN, G., 1999. Neo-gene sapropels in the Mediterranean: a review. *Mar. Geol.,* 153, 11-28.

DE LANGE, G.J., JARVIS, I., & KUIJPERS, A., 1987. Geochemical characteristics and provenance of late Quaternary sediments from the Madeira Abyssal Plain, N Atlantic. In: P.P.E., Weaver & J., Thomson (Eds) Geology and geochemistry of abyssal plains. *Geological Special Publication*, 31, pp.147-165.

DAVIS, J.C., 1986. Statistics and data analysis in geology. J. Wiley & Sons, New-York, 646p.

DRUITT, T.H., EDWARDS, L., MELLORS, R.M., PY-

LE, D.M., SPARKS, R.S.J., LANPHERE, M., DAVIES, M., & BARREIRO, B., 1999. Santorini volcano. *Geological Society, London, Memoirs,* 19, 169p.

DYMOND, J., SUESS, E., & LYLE, M., 1992. Barium in deep-sea sediment: a proxy for paleproductivity. *Paleoceanography*, 7 2, 163-181.

EMELYANOV, E.M., MITROPOLSKY, A.Y., SHIMKUS, K.M., & MOUSSA, A.A., 1979. Geochemistry of the Mediterranean Sea. *Kiev. Naukova, Dumka,* 133p.

EMELYANOV, E.M., & SHIMKUS, K.M., 1986. Geochemistry and sedimentology of the Mediterranean Sea. Reidel. Publ. Co., 553p.

GARBE-SCHONBERG, C.D. 1993. Simultaneous determination of 37 trace elements in 28 international rock standards by ICP-MS. *Geostandards Newsletter,* 17, 81-93

GOLDBERG, E.D., & ARRHENIUS, G.O.S., 1958. Geochemistry of Pacific pelagic sediments. *Geochim. Cosmochim. Acta*, 13, 153-212.

GOREAU, T.J., 1977. Coral skeletal chemistry; physiological and environmental regulation of stable isotopes and trace metals in Monastrea annularis. *Proc. R. Soc. Lond.,* B, 196, 291-299.

HERMAN, Y., 1972. Quaternary eastern Mediterranean sediments: Micropaleontology and climatic record. In: D.J., Stanley (Ed), The Mediterranean Sea: A natural sedimentation laboratory. Dowden, Hutchinson & Ross, Inc., Stroudsburg, Pennsylvania, 129-147.

HIRST, D.M., 1962. The geochemistry of modern sediments from the Gulf of Paria - I. *Geochim. Cosmochim. Acta*, 26, 309-334.

HODKINSON, R.A., & CRONAN, D.S., 1991. Geochemistry ofrecent hydrothermal sediments in relation to tectonic environment in the Lau Basin, southwest Pacific. *Mar. Geol.*, 98, 353-366.

HODKINSON, R.A., CRONAN, D.S., VARNAVAS, S., & PERISSORATIS, C., 1994. Regional geochemistry of sediments from the Hellenic volcanic arc in regard to submarine hydrothermal activity. *Mar. Georesources Geotechnol.*, 12, 83-129.

JACKSON, J.A., 1994. Active tectonics of the Aegean region. *Annu. Rev. Earth Planet. Sci.*, 22, 239-271.

KARAGEORGIS, A., 1992. Mineralogical, Geochemical & Stratigraphic study of the Holoce cover in the marine area between Attica-Euboea-N. Cyclades.Ph.D.Thesis,Univ.Thessaloniki, 20, 200p.

KARAGEORGIS A., ANAGNOSTOU CH, SIOULAS A., KASSOLI-FOURNARAKI A., & ELEFTHERIADIS, G., 1997. Sedimentology and geochemistry of surface sediments in a semi-enclosed marine area. Central Aegean - Greece. *Ocean. Acta,* 20 (3), 513-520.

KARAGEORGIS, A., ANAGNOSTOU, CH., SIOULAS, A., CHRONIS, G., & PAPATHANASSIOU, E., 1998. Sediment geochemistry and mineralogy in Milos bay, SW Kyklades, Aegean Sea-Greece. *J. Mar. Syst.,* 16/3-4, 269-281.

KELLER, J., RYAN, RYAN, W.B.F., NINKOVICH,D., & ALTHERR, R., 1978. Explosive volcanic activity in the Mediterranean over the past 200,000 yr as recorded in deep-sea sediments. *Geol. Soc. Am. Bull.*, 89, 591-604.

KEMP, A.L.W., THOMAS, R.L., & MUDROCHOVA, A., 1974. Sedimentation rates and recent sediment history of Lakes Ontario, Erie and Huron. *J. Sedim. Petrol.,* 44, 207-218.

KIDD, R.B., CITA, M.B., & RYAN, W.B.F., 1978. Stratigraphy of eastern Mediterranean sapropel sequences recovered during Leg 42A and their paleoenvironmental significance. Init.Rep. DSDP 42A, 421-443.

KNOX, R.W.O'B., 1993. Tephra layers as precise chronostratigraphical markers. In: E.A., Hailwood, & R.B., Kidd (Eds), High resolution stratigraphy. *Geological Society Special Publication* 70, London, pp. 169-186.

KULLENBERG, B., 1952. On the salinity of water contained in marine sediments. *Medd. Oceanogr. Inst. Goteborg*, 21, 1-38.

LYKOUSIS, V., ANAGNOSTOU, C., PAVLAKIS, P., ROUSAKIS, G., & ALEXANDRI, M., 1995. Quaternary sedimentary history and neotectonic evolution of the eastern part of central Aegean Sea, Greece. *Mar. Geol.*, 128, 59-71.

MCCOY, F.W., 1974. Late Quaternary Sedimentation in the Eastern Mediterranean Sea. Unpubl. Ph.D. Thesis, Harvard Univ., 132 pp.

MCCOY, F.W., 1981. Aerial distribution, redeposition and mixing of tephra within deep-sea sediments of the eastern Mediterranean Sea. In: S., Self & R.S.J., Sparks (Eds), Tephra studies. Reidel Publ. Co., pp. 245- 254.

MELLIS, O., 1954. Volcanic-ash horizons in deep-sea sediments from the eastern Mediterranean. *Deep-Sea Res.*, 2, 89-92.

MURPHY, E., MCMURTRY, G.M., HYUN KIM, K., & DECARLO, E.H., 1991. Geochemistry andgeochronology of a hydrothermal fer romanganese deposit from the North Fiji Basin. *Mar. Geol.*, 98, 297-312.

NATH, B.N., RAO, V.P., & BECKER, K.P., 1989. Geochemical evidence of terrigenous influence in deep-sea sediments up to 8 deg. S in the central Indian basin. *Mar. Geol.,* 87, 301-313.

NINKOVICH, D., & HEEZEN, B.C., 1967. Physical and chemical properties of volcanic glass shards from Pozzolana ash, Thera Island, and from upper and lower ash layers in eastern Mediterranean deep-sea cores. *Nature*, 213, 582-584.

OLAUSSON, E., 1961. Studies in deep-sea cores. *Rep. Swed. Deep-Sea Exped.* 1947-1948, 8,337-391.

PETERMAN, Z.E., & HEDGE, C., 1974. Strontium. Isotopes in Nature. In: K.H., Wedepohl (Ed), Handbook of geochemistry. Springer-Verlag, Berlin, 38-B, 1-14.

PICHLER, H., & FRIEDRICH, W., 1976. Radiocarbon dates of Santorini volcanics. *Nature*, 262, 373-374.

POULOS, S.E., LYKOUSIS, V., COLLINS, M.B., ROHLING, E.J., & PATTIARATCHI, C.B., 1999. Sedimentation processes in a tectonically active environment: the Kerkyra-Kefalonia submarine valley system NE Ionian Sea. *Mar. Geol.,* 160, 25-44.

ROHLING, E.J., 1994. Review and new aspects concerning the formation of eastern Mediterranean sapropels. *Mar. Geol.,* 122, 1-28.

SACCANI, E., 1987. Double provenance of sand-size sediments in the southern Aegean forearc basin. *J. Sedim. Petrol.*, 57, 736-745.

SHANKAR, R., SUBARRAO, K. V., & KOLLA, V., 1987. Geochemistry of surface sediments from the Arabian Sea. *Mar. Geol.,* 76, 253-279.

SHIMKUS, K.M., 1981. Sedimentation of the Mediterranean Sea during Late Quaternary time. M.: *Nauka*, 240p. (in Russian).

SUTHERLAND, H., CALVERT, S.E., & MORRIS, R.J., 1984. Geochemical Studies of the recent sapropel and associated sediments from the Hellenic Outer Ridge, eastern Mediterranean Sea, I. Mineralogy and chemical composition. *Mar. Geol.*, 56, 79-92.

THOMSON, J., HIGGS, N.C., WILSON, T.R.S., CRODUACE, I.W., DE LANGE, G.J., & VAN SANTVOORT, P.J.M., 1995. Redestribution and chemical behaviour of redox-sensitive elements around S1, the most recent eastern Mediterranean sapropel. *Geochim. Cosmochim. Acta.*, 59, 3487-3501.

THOMSON, J., MERCONE, D., DE LANGE, G. J., & VAN SANTVOORT, P.J.M., 1999. Review of re-cent advances in the interpretation of eastern Mediterranean sapropel S1 from geochemical evi dence. *Mar. Geol.,* 153, 77- 89.

THUNELL, R., FEDERMAN, A., SPARKS, S., & WILLIAMS, D., 1979. The age, origin, and volcanological significance of the Y-5 ash layer in the Mediterranean. *Quat. Res.,* 12, 241-253.

TUREKIAN, K.K., 1964. The marine geochemistry of strontium. Geochim. *Cosmo-chim. Acta,* 28, 1479-1483.

TUREKIAN, K.K., 1974. Strontium. Abundance in Common Sediments and Sedimentary Rocks. In: K.H., Wedepohl (Ed), Hand-book of Geochemistry. Springer-Verlag, Berlin, 38-K, 1-13.

VARNAVAS, S.P., PANAGIOTARAS, D., & MEGALOVASILIS, P.S., 1998. Chemical characteristics of a submarine hydrothermal system offshore Kos Island, on the Hellenic volcanic arc. *Rapp.Comm. Int. Mer Medit.,* 35, 104-105.

VEIZER, J., & WENDT, J., 1976. Mineralogy and chemical composition of Recent and fossil skeletons of calcareous sponges. *Neues Jahrb. Geol. Paleontol. Monatsh.*, 9, 558-568.

VERGNAUD-GRAZZINI, C., 1985. Mediterranean late Cenozoic stable isotope record: stratigraphic and paleoclimatic implications. In: D.J., Stanley & F.C., Wezel (Eds), Geological Evolution of the Mediterranean Basin. Springer, New York, pp. 413-451.

VINCI, A., 1985. Distribution and chemical composition of tephra layers from eastern Mediterranean abyssal sediments. *Mar.Geol.*, 64,143-155.

VINCI, A., 1987. The "Cape Riva tephra layer" Y-2 (Santorini volcano) in deep-sea sediments from eastern Mediterranean Sea. *Boll. Ocean. Teor. Appl.*, 5(2), 117-123.

WATKINS, N.D., SPARKS, R.S.J., SIGURDSSON, H., HUANG, T.C., FEDERMAN, A., CAREY, S., & NINKOVICH, D., 1978. Volume and extent of the Minoan tephra from Santorini volcano: new evidence from deep-sea sediment cores. *Nature*, 271, 122-126.

WEHAUSEN, R., & BRUMSACK, H.-J., 1999. Cyclic variations in the chemical composition of eastern Mediterranean Pliocene sediments: a key for understanding sapropel formation. *Mar. Geol.*, 153, 161-176.

WINDOM, H.L., SCHROPP, S.J., CALDER, F.D., RYAN, J.D., SMITH, R.G., JR., BURNEY, J.C., LEWIS, G.G., & RAWLINSON, C.H., 1989. Natural trace metal concentrations in estuarine andcoastal marine sediments of the southeastern U.S. E*nviron. Sci. Technol.*, 23, 314-320.